Colloid Polym Sci 279:1169–1176 (2001)

ORIGINAL CONTRIBUTION

J. E. K. Schawe
I. Alig

Heat capacity relaxation during polymer network formation: limitations of equlibria descriptions

Received: 29 August 2000
Accepted: 28 May 2001

J. E. K. Schawe (✉)
Mettler-Toledo GmbH
Sonnenbergstrasse 74
8603 Schwerzenbach, Switzerland
e-mail: juergen.schawe@mt.com
Tel.: +41-1-8067438
Fax: +41-1-8067240

I. Alig
Deutsches Kunststoff-Institut
Schlossgartenstrasse 6
64289 Darmstadt, Germany

Abstract During macromolecular growth (e.g. polymerization or curing) irreversible changes occur in the material. In addition, the material can transform from a liquid into a glassy state. This process can be investigated by measuring the specific complex heat capacity relaxation during the isothermal reaction. The increase of the characteristic relaxation time during the reaction is a measure of changes in the molecular dynamics during the course of the reaction. Because of the feedback of the relaxation processes on the reaction kinetics a thorough understanding of the relaxation behavior is essential to understand fully the properties of thermosetting systems. Starting from a description of the relaxation of a chemically stable material, an equilibrium approach for the thermal relaxation during the reaction is developed and the limits of this approach are discussed. Experimental values of the characteristic relaxation time measured during network formation of an epoxy thermoset are shown to deviate considerably from those predicted by the equilibrium extension approach after vitrification. To describe the thermal relaxation during isothermal vitrification by polymerization we suggest introducing a fictive temperature and a reduced time scale in the equilibrium model.

Key words Epoxy thermoset · Vitrification · Relaxation · Heat capacity · Temperature-modulated differential scanning calorimetry

Introduction

To fully understand the curing behavior of thermosets (or isothermal macromolecular growth) it is essential to have greater insight into the interactions between relaxation processes and the chemical reaction. Dynamic mechanical and dielectric techniques are frequently used for investigation of relaxation processes during chemical reactions [1]. Conventional differential scanning calorimetry (DSC) delivers information on the time or temperature dependence of conversion and on vitrification owing to the glass transition. During isothermal reaction at the reaction temperature, T_{react}, the glass-transition temperature, T_g, of the reacting mixture increases irreversibly. If the value of T_g approaches T_{react} the system vitrifies and both relaxation and reaction kinetics slow dramatically [2, 3]. A limitation of the conventional DSC technique is that the thermal relaxation cannot be measured directly during the chemical reaction. Gobrecht et al. [4] measured the heat flow of the reaction and the heat capacity change during the reaction simultaneously using temperature-modulated DSC (TMDSC). Using this technique, thermal relaxation can be separated from the heat of reaction and measured during isothermal reaction. This type of experiment was first performed by Cassettari et al. [5]. Ferrari et al. [6] proposed a description of the thermal relaxation which

was based on a conversion-time-dependent or reaction-time-dependent relaxation time and a structure-independent relaxation function.

Van Assche et al. [7] used the heat capacity change during the reaction measured by TMDSC to determine a mobility factor that describes the amount of vitrification during the reaction and that can be used to model the change from a chemically controlled into a diffusion-controlled reaction. Following this interpretation, the heat capacity change during the reaction measured by TMDSC represents the vitrification process or, in other words, the discrepancy between the actual reacting mixture and a physically equilibrated liquid. The relation between heat capacity changes and molecular relaxation processes is not considered in this model.

In this article we present an approach for describing the thermal relaxation during isothermal network formation on the basis of models developed for the description of the main (or α-) relaxation in an equilibrated, chemically stable material. The predictions of this equilibrium approach are compared to experimental results of investigations into the relaxation of the specific heat capacity during isothermal curing of an epoxy thermoset. The limits of validity of such an ''equilibrium model'' for vitrification of a liquid into a nonequilibrated glassy state during macromolecular growth are discussed and an extension of the approach is suggested.

Experimental

Samples

Diglycidylether of bisphenol A (DGEBA) supplied by the Shell Chemical Company (Epikote 828) and diaminodiphenyl methane (DDM) supplied by Aldrich were used for the sample preparation. Details of the reaction mechanism are described in Refs. [8–12]. DGEBA and DDM were heated separately to 120 °C. The substances were mixed in stoichiometric amounts at 120 °C and stirred for 20 s. The mixture was then rapidly cooled to room temperature and a sample of 2.875 mg was filled into an aluminum crucible. The measurement was performed immediately after the sample preparation. In order to prepare the finally cured material the samples were heated to 200 °C at approximately 5 K/min and were annealed for 20 min.

Methods

The quasiisothermal TMDSC measurements were performed using a Mettler Toledo DSC 821^e with an intracooler using the ADSC software option for temperature modulation. The instrument was temperature-calibrated with water, indium and tin. Indium was used for the heat-flow calibration. The furnace atmosphere was defined by 50 ml/min of nitrogen. Conventional DSC measurements were performed in a temperature range from −45 to 230 °C with a heating rate of 10 K/min.

Before performing the quasiisothermal curing measurement, the DSC furnace was heated to the curing temperature (T_{react} = 100 °C). The sample was placed into the furnace using a sample robot. Nonetheless, the sample was at room temperature for no longer than 2 min.

In the TMDSC measurements the temperature program is given by

$$T(t) = T_{react} + T_a \sin \omega_0 t \ , \quad (1)$$

where T_{react} is the curing temperature and T_a is the temperature amplitude. ω_0 is the angular frequency ($\omega_0 = 2\pi f_0 = 2\pi/t_p$). A T_a of 0.5 K was used. The period, t_p, was 24 s ($f_0 = 41.7$ mHz). The measuring time was approximately 10 ks. An empty pan was run under the same conditions for reference. Blank corrected data (empty pan run subtracted from sample run) were used for all the calculations.

The measured heat-flow rate can be separated into two components, Φ_u and Φ_p. The underlying component of the heat-flow rate, Φ_u, is determined by the moving average over one period and corresponds to the conventional DSC signal. Φ_u is proportional to the reaction rate:

$$\Phi_u(t) = m\Delta h_r \frac{d\xi}{dt} \ , \quad (2)$$

where m is the sample mass, Δh_r the specific enthalpy of reaction and ξ the conversion. The difference between the measured heat-flow rate, $\Phi(t)$, and $\Phi_u(t)$ is the periodic component of the heat flow $\Phi_p(t) = \Phi(t) - \Phi_u(t)$. Fourier analysis of the periodic component yields the first harmonic:

$$\Phi_p^{(1)}(t) = \Phi_a \cos(\omega_0 t - \varphi) \ , \quad (3)$$

where Φ_a is the amplitude of the periodic component of the heat-flow rate and φ the phase shift.

The phase shift is affected by the rate of reaction ($d\xi/dt$), the heat capacity of the sample and by the heat transfer conditions. Details of the calibration procedure are given elsewhere [13].

The real c' and the imaginary part c'' of the complex specific heat capacity c^* is then defined by

$$c' = |c^*| \cos \varphi \quad (4)$$

and

$$c'' = |c^*| \sin \varphi \ , \quad (5)$$

where $|c^*| = \frac{\Phi_a}{m\omega_0 T_a} = \sqrt{c'^2 + c''^2}$ is the modulus of the complex heat capacity, $c^* = c' - ic''$ $\left[i = (-1)^{0.5}\right]$.

The glass-transition temperature of the pure epoxy resin and the fully cured material was measured using TMDSC in a frequency range between 5.6 and 66.7 mHz at an underlying cooling rate of 0.1 K/min. The glass-transition temperature was determined as the temperature of the half step height of the c' step.

Dielectric relaxation spectroscopy was performed in a frequency range from 3 Hz to 1.5 MHz by using a dielectric setup from NOVOCONTROL. Details of the data analysis are described elsewhere [14].

Results and discussion

Experimental data

The underlying heat flow signal, Φ_u, is shown together with the real (c') and imaginary part (c'') of the complex specific heat capacity during an isothermal reaction of the epoxy thermoset (DGEBA/DDM) at 100 °C in Fig. 1.

The underlying heat flow signal reflects the heat of reaction. This curve shows an exothermal peak at about 20 min. For reaction times longer than 60 min

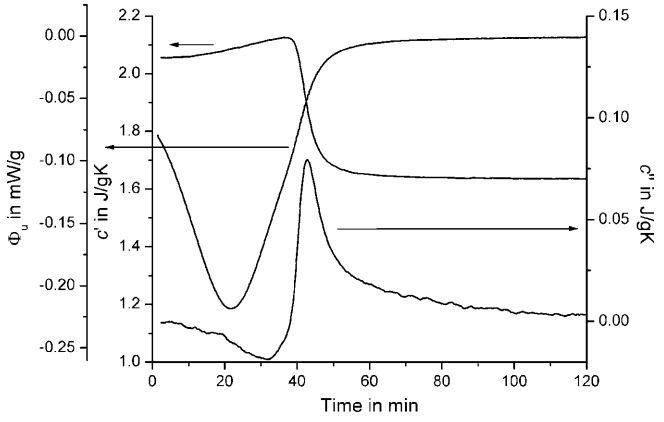

Fig. 1 Real and imaginary part of the specific complex heat capacity and the underlying heat flow component during isothermal curing of the thermoset (diglycidylether of bisphenol A, *DGEBA*/diaminodiphenyl methane, *DDM*) at 100 °C and a modulation frequency of 41.7 mHz

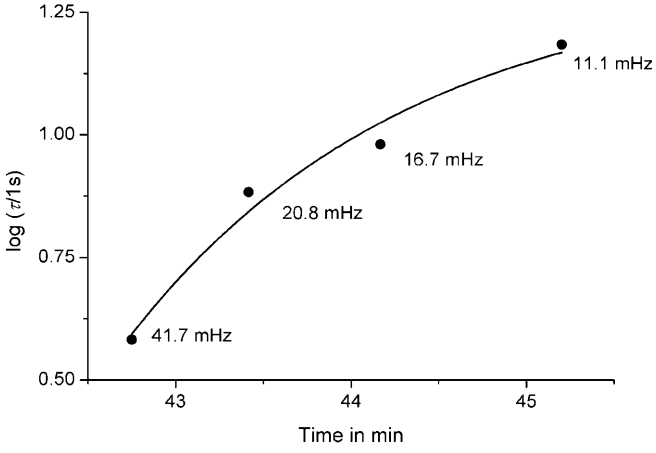

Fig. 2 Change in the thermal relaxation time with time during the reaction measured at a reaction temperature of 100 °C in a frequency range between 10 and 42 mHz

no significant heat flow related to the reaction can be detected. The real part of the complex heat capacity increases slightly at short reaction times ($t_{react} <$ 40 min). In this time interval the heat capacity measured is related to the liquid state. The almost linear increase in c' with time during the initial interval of curing seems to reflect an increase in the specific heat capacity owing to an increase in configurational and/or vibrational contributions in the liquid state originating from network growth [6]. The sharp decrease after about 35 min represents a reduction in the degree of freedom of the system owing to an irreversible structure change from a liquid to a glassy solid. In the glassy polymer network the specific heat capacity becomes nearly constant. The inflection point of the stepwise decrease in c' occurs at about 43 min and corresponds to an isothermal vitrification time where the main glass-to-rubber relaxation freezes for a given frequency. The step in c' is related to the maximum in c'', which represents a situation where the characteristic relaxation time, τ, of the molecular rearrangement becomes comparable to the inverse of the angular frequency, ω_0, of the temperature modulation ($\omega_0\tau = 1$). The relaxation time as a function of the curing time, t_{react}, was estimated by using the assumption $\omega_0\tau = 1$ for the maximum in the $c''(t_{react})$ curves (similar to Fig. 1) measured at 11.1, 16.7, 20.8 and 41.7 mHz (periods of 24, 48, 60 and 90 s) and is shown in Fig. 2.

As expected, the relaxation time increases with the reaction time, reflecting the fact that the vitrification time measured by TMDSC is frequency-dependent. This behavior can be understood as a relaxation process shifting to lower frequencies during a chemical reaction, i.e. a reaction-time-dependent relaxation.

Chemically induced relaxation process

The time-dependent behavior of complex heat capacity during an isothermal reaction can be understood as a thermal relaxation process irreversibly shifting to lower frequencies. For better understanding, a simplified picture of changes in thermal relaxation behavior during network formation or polymer growth is shown in Fig. 3.

The cooperative thermal relaxation (main or α-relaxation) in a liquid can be described by a curved line in the activation diagram [15, 16]. The two dashed lines represent the traces in the activation diagram of the initial mixture ($\xi = 0$) and the fully cured material

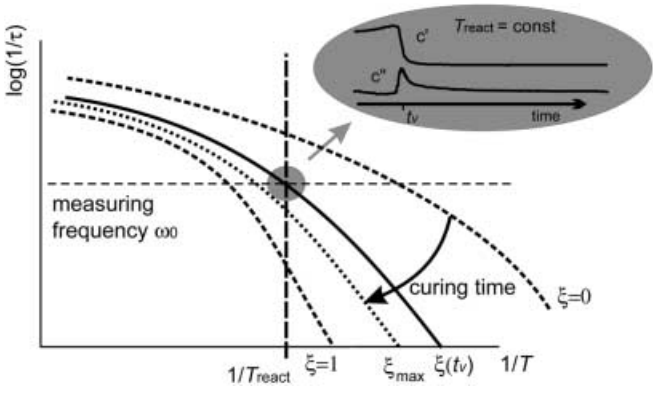

Fig. 3 Schematic representation of the change in the relaxation curve during a chemical reaction. The characteristic relaxation times $\tau(T)$ are plotted for different degrees of conversions, ξ, in an activation plot. The *dashed lines* for $\xi = 0$ and $\xi = 1$ represent the initial and final conversion, respectively. The *solid line* characterizes the relaxation behavior of a material with a characteristic relaxation time τ (T_{react}) $= 1/\omega_0$. T_{react} is the curing temperature and ω_0 is the probe frequency. The *dotted line* represents the activation curve for long curing at T_{react}

($\xi = 1$), respectively. At T_{react} the maximum conversion is ξ_{max} (< 1) (dotted line). The experimental conditions given by T_{react} and the modulation frequency, ω_0, define the state of the isothermally reacting mixture in the activation diagram. During the reaction the glass temperature shifts to a higher temperature and the relaxation time decreases irreversibly; therefore, the activation curve shifts with increasing conversion from the curve of the initial mixture more and more towards the curve of the fully cured material. In the case where the actual relaxation frequency, $1/\tau$, at T_{react} is larger than the probe frequency, ω_0, the behavior of a liquid is reflected in the measurements. In a relaxation experiment with a probe frequency ω_0 during isothermal polymerization at T_{react} the vitrification time, t_v, is defined by $\omega_0\tau(\xi, T) = 1$, which is depicted in the activation diagram (Fig. 3) by the crossing of the actual relaxation curve for $\xi(t_v)$ to the experimental conditions (T_{react}, ω_0). This situation is related to the step in $c'(t)$ and the maximum in $c''(t)$ for a given reaction temperature and frequency.

If a lower experimental frequency is chosen, the relaxation process will be measured at a longer reaction time; therefore we have to understand t_v as a frequency-dependent, apparent vitrification time. The reason for the measured transition in the thermal relaxation behavior is the change in the molecular dynamics owing to irreversible network formation. This simplified picture of thermal relaxation during an isothermal reaction includes the basic ideas of the following quantitative description.

The reaction-time dependence of the relaxation time

For chemically stable materials in thermal equilibrium the temperature dependence of τ can be expressed by the Vogel–Fulcher (VF) equation [17, 18]:

$$\tau = \tau_0 \exp\left(\frac{B}{T - T_v}\right) \quad , \tag{6}$$

where B is the curvature parameter, T_v the Vogel temperature and τ_0 the minimum relaxation time. T_v can be estimated experimentally from T_g (typically measured by DSC with scanning rates of 10 K/min):

$$T_v = T_g - C_2 \quad , \tag{7}$$

where C_2 is a constant (Williams–Landel–Ferry constant).

The fully cured material and the pure epoxy resin can be considered to be chemically stable materials. Using DSC and TMDSC measurements it was shown that the glass-transition temperature of pure epoxy resin and its mixture with the cross-linker are identical within the error limits; therefore, we assume that the activation curve of the epoxy resin represents the relaxation time temperature dependence of the initial mixture. The relaxation behavior of both the fully cured material and the pure epoxy resin was measured in a frequency range from 3 Hz to 1.5 MHz by dielectric spectroscopy. The frequency dependence of the complex dielectric permittivity measured at different temperatures was analyzed using the Havriliak–Negami (HN) function [19] to estimate the characteristic relaxation times, τ. The thermal relaxation times were estimated from TMDSC data measured in a frequency range between 66.7 and 5.6 mHz applying the assumption $\omega_0\tau = 1$. Using this data, the VF parameters B, τ_0 and C_2 can be determined by a combination of Eqs. (6) and (7). The glass-transition temperature of the unreacted ($\xi = 0$) and the fully cured ($\xi = 1$) material was determined by DSC for a cooling rate of 10 K/min to be 255 and 435 K, respectively. For the sake of simplification we assume that only T_v in the VF equation depends on the conversion and that C_2 is constant during curing. These assumptions are consistent with earlier investigations [20]. The VF parameter was determined to be $B = 983.2$, $\tau_0 = 2.46 \times 10^{-14}$ s and $C_2 = 26.5$ K by fitting the dielectric and TMDSC data together (Fig. 4). The same set of parameters shows an adequate fit for both pure epoxy resins without cross-linker and the fully cured sample. The value of C_2 is relatively small; however, it corresponds to the difference between T_g and the Vogel temperature determined from kinetic investigations of curing processes (between 25 and 35 K) [21, 22]. For the determination of the fit parameter C_2 we combined

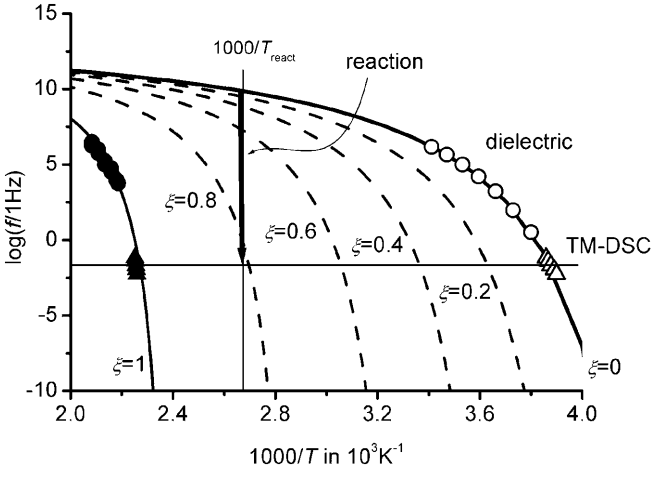

Fig. 4 Activation diagram of the thermoset (DGEBA/DDM) measured by dielectric spectroscopy (*circles*) and temperature-modulated differential scanning calorimetry (*TMDSC*) (*triangles*). The *open symbols* represent the initial system ($\xi = 0$) and the *filled symbols* mark the fully cured material ($\xi = 1$). These data are fitted by a Vogel–Fulcher equation (*continuous curves*). The *arrow* describes the change in the relaxation time during a reaction at 100 °C. The *broken curves* are calculated from the Vogel–Fulcher parameters and the conversion-dependent glass-transition temperature for different conversions (see Fig. 5)

calorimetric and dielectric data. A small deviation in the temperature calibration or little differences in the traces in the activation diagram measured by the two techniques are possible. This could be the origin of the small value of C_2.

If the change in the glass-transition temperature as a function of conversion is known, the VF curves for each conversion can be calculated from Eqs. (12) and (13); this is shown in Fig. 5. The dependence of T_g on ξ is measured for samples cured at different reacting times by conventional DSC. As shown in Fig. 5, one possible approximation of the experimental data is the DiBenedetto equation [23, 24]:

$$T_g(\xi) = \frac{\lambda\,\xi\left(T_{g1} - T_{g0}\right)}{1-(1-\lambda)\xi} + T_{g0} \quad , \tag{8}$$

where T_{g0} and T_{g1} are the glass temperatures of the material for $\xi = 0$ and $\xi = 1$. λ is determined to be 0.4.

During the isothermal reaction the conversion changes continuously with time. The conversion as a function of the reaction time $\xi(t_{react})$ can be determined directly from the underlying heat-flow rate, $\Phi_u(t_{react})$:

$$\xi(t_{react}) = \frac{1}{m\Delta h_r}\int_0^{t_{react}} \Phi_u(t')\mathrm{d}t' \quad , \tag{9}$$

where Δh_r is the specific heat of reaction. From DSC measurements we obtained $\Delta h_r = 406$ J/g. The reaction-time dependence of the glass-transition temperature and the Vogel temperature can be calculated by insertion of Eq. (9) into Eqs. (8) and (7). An expression for the reaction-time dependence of the relaxation time follows from the VF equation (Eq. 6):

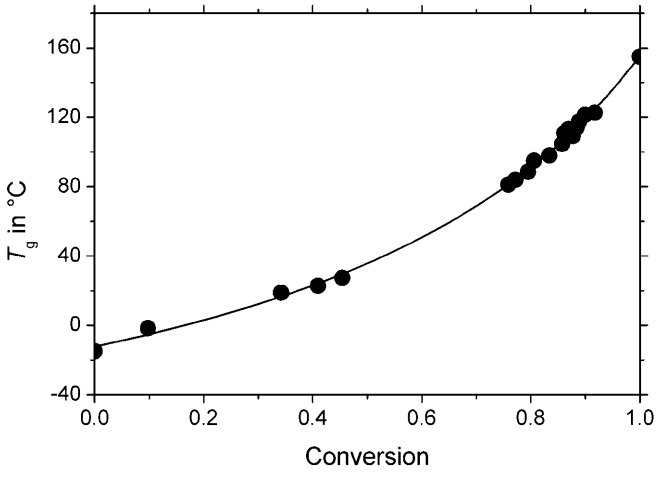

Fig. 5 Glass-transition temperature as a function of conversion. The *solid line* represents the DiBenedetto equation

$$\tau(t_{react}) = \tau_0 \exp\left(\frac{B}{T_{react} + C_2 - T_g[\xi(t_{react})]}\right) \quad . \tag{10}$$

During a curing reaction the characteristic relaxation time strongly depends on the conversion, ξ. With increasing conversion the relaxation processes become extremely slow and τ increases by several orders of magnitude (see the arrow in Fig. 4).

The relaxation function and complex heat capacity

For a structurally stable material the frequency dependence of $c^*(\omega)$ can be expressed by a relaxation function, $\phi(t)$:

$$c^*(\omega) = c_\infty + \Delta c \int_0^\infty \frac{\mathrm{d}\phi(t)}{\mathrm{d}t}\exp(-\mathrm{i}\omega t)\mathrm{d}t \quad , \tag{11}$$

with $\Delta c = c_0 - c_\infty$, where c_0 and c_∞ are the low- and high-frequency limiting values of c', respectively.

A commonly used empirical relaxation function $\phi(t)$ is the stretched exponential Kohlrausch–Williams–Watts (KWW) function [25, 26]:

$$\phi(t) = \exp\left[-\left(\frac{t}{\tau}\right)^{\beta_{KWW}}\right] \quad , \tag{12}$$

where τ is the characteristic relaxation time and β_{KWW} is a shape parameter ($0 < \beta_{KWW} \leq 1$). With the Fourier transform of $\mathrm{d}\phi/\mathrm{d}t$

$$\psi(\omega,\tau) = \int_0^\infty \frac{\mathrm{d}\phi(t,\tau)}{\mathrm{d}t}\exp(-\mathrm{i}\omega t)\mathrm{d}t \tag{13}$$

one rewrites Eq. (11) as

$$c^*(\omega,\tau) = c_\infty + \Delta c \quad \psi(\omega,\tau) \quad . \tag{14}$$

In the present article the frequency-dependent heat capacity is discussed; therefore the function $\psi(\omega,\tau)$ must be used instead of the relaxation function. For simplification of the mathematical structure of the equation an analytic expression for $\psi(\omega,\tau)$ is useful. A very flexible empirical function for $\psi(\omega,\tau)$ is the HN function [19, 27], which is usually applied for dielectric relaxation experiments:

$$\psi(\omega,\tau) = \psi'(\omega,\tau) - \mathrm{i}\psi''(\omega,\tau) = \frac{1}{\left[1+(\mathrm{i}\omega t)^\beta\right]^\gamma} \quad , \tag{15}$$

with

$$\psi'(\omega,\tau) = \frac{\cos\left[\gamma\ \arctan\left(\frac{(\omega\tau)^\beta \sin(\pi\beta/2)}{1+(\omega\tau)^\beta\cos(\pi\beta/2)}\right)\right]}{\left[1+2(\omega\tau)^\beta\cos(\pi\beta/2)+(\omega\tau)^{2\beta}\right]^{\gamma/2}} \tag{16}$$

and

$$\psi''(\omega,\tau)=\frac{\sin\left[\gamma\ \arctan\left(\frac{(\omega\tau)^{\beta}\sin(\pi\beta/2)}{1+(\omega\tau)^{\beta}\cos(\pi\beta/2)}\right)\right]}{\left[1+2(\omega\tau)^{\beta}\cos(\pi\beta/2)+(\omega\tau)^{2\beta}\right]^{\gamma/2}}\ , \qquad (17)$$

where β and γ are shape parameters. In order to calculate the complex specific heat capacity the relaxation strength, Δc, and the HN parameters, β and γ, are needed.

For our calculations the curing-time dependence of Δc was estimated from the c' curve in Fig. 1. We assumed that

$$\Delta c(t_{\mathrm{react}})=c_0+at_{\mathrm{react}}-c_{\infty}\ , \qquad (18)$$

where $c_0 + at_{\mathrm{react}}$ ($c_0 = 2.0$ J/gK, $a = 2.3$ mJ/gKmin) and $c_{\infty} = 1.65$ J/gK are the low- and the high-frequency limiting values of $c'(\omega)$.

Data gathered from dielectric spectroscopy were used to determine the HN parameters. Unfortunately, the direct determination of these parameters for fully cured material was not possible owing to high direct current conductivity. However, in dielectric measurements [28] on a DGEBA network it was shown that the shape of $\psi(\omega,\tau)$ is almost independent of the degree of reaction between $0.66 \le \xi \le 1.0$ and the parameter β_{KWW} was reported to be between 0.48 and 0.37.

From this parameter we estimated the HN parameters $\beta = 0.6$ and $\gamma = 0.5$ using the procedure described in Ref. [29]. Combining the reaction-time dependence of the relaxation time (Eqs. 10, 15) with Eq. (14) yields the curing-time dependence of the complex specific heat capacity:

$$c^*(\omega_0,t_{\mathrm{react}})=c_{\infty}+\frac{c_0+at_{\mathrm{react}}}{\left\{1+\mathrm{i}\left[\omega_0\tau_0\exp\left(\frac{B}{T_{\mathrm{react}}-T_{\mathrm{g}}[\xi(t_{\mathrm{react}})]+C_2}\right)\right]^{\beta}\right\}^{\gamma}}\ . \qquad (19)$$

All the parameters used for modeling $c^*(t_{\mathrm{react}})$ summarized in Table 1 are estimates based on data obtained from independent experiments.

A comparison of the calculated curves (dashed line) with the experimental data is shown in Fig. 6. The calculated and measured curves are generally in good agreement; however, compared to the measured curves the shape of the calculated c' and c'' curves is narrower and the maximum in c'' and the step in c' are at shorter curing times for the calculated curves.

The fundamental difficulties of the equilibrium model are more evident in the time evolution of the characteristic relaxation time (Fig. 7). For long curing times the model presented (see Eq. 10) yields completely unrealistic relaxation times (10^{37} s at $t_{\mathrm{react}} = 60$ min). A comparison between the measured relaxation times and the results of the equilibrium approach shows that the

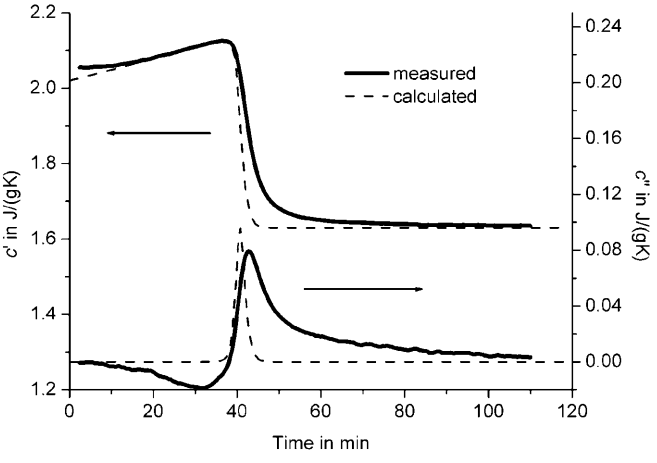

Fig. 6 Measured (*solid line*) and calculated curves (*dashed lines*) of the real and imaginary part of the specific complex heat capacity for the epoxy thermoset versus reaction time

Table 1 Parameters used for model calculation

Equation	Parameter	Value	Experimental method
	ω_0	0.262 1/s	Temperature-modulated differential scanning calorimetry
2	Δh_{r}	406 J/g	Differential scanning calorimetry
(12, 18)	τ_0	2.46×10^{-14} s	Dielectric and temperature-modulated differential scanning calorimetry
(12, 18)	B	983.2 K	
(13, 18)	C_2	26.5 K	Dielectric and temperature-modulated differential scanning calorimetry
(10, 18)	β	0.6	Dielectric
(10, 18)	γ	0.5	
(14)	$T_{\mathrm{g},0}$	255 K	Differential scanning calorimetry
(14)	$T_{\mathrm{g},1}$	435 K	
(14)	λ	0.4	
(19)	c_0	2.0 J/gK	Temperature-modulated differential scanning calorimetry
(19)	a	2.3 mJ/gKmin	
(19)	c_{∞}	1.65 J/gK	

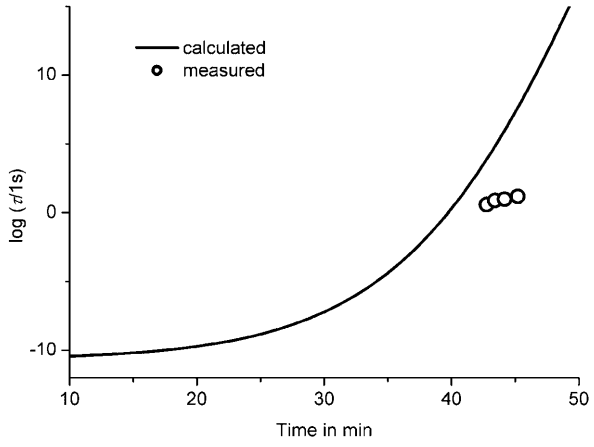

Fig. 7 Time evaluation of the relaxation time during a reaction at 100 °C. The *line* shows the results from the equilibrium approach; the circuits represent the measured data from Fig. 2

measured τ values in the reaction time interval of investigation (42 min $\leq t_{react} \leq$ 45 min) are between 3 and 7 decades below the calculated relaxation times. This is an indication of the limitations of the simple model presented without taking into consideration the freezing of structural relaxation during vitrification by reaction.

An extrapolation of the experimental relaxation times to shorter reaction times in Fig. 7 suggests a deviation from the calculated line at about 40 min. Before this time the relaxation behavior of the reacting system is like an equilibrated liquid. At about 40 min, thermal relaxation becomes influenced by a nonequilibrium situation owing to freezing. This behavior of the relaxation time during isothermal network formation is similar to that observed during cooling of a chemically stable liquid in the glass-transition region. Since a so-called fictive temperature can describe such a cooling experiment, an analog approach should be possible for describing vitrification by chemical reaction. In this picture the fictive temperature is a measure of the relaxation of the entropy (structure) in temperature units. A nonequilibrium approach using the concept of a fictive temperature for the description of isothermal vitrification by network formation is in progress.

Conclusion

Vitrification during isothermal polymer network formation (linear chain growth) can be divided into two strongly interactive processes: an irreversible chemical reaction, described by the conversion $\xi(t_{react})$, on the one hand, and the structural and thermal relaxation behavior characterized by a decrease in the characteristic relaxation times and an increase in the glass-transition temperature with increasing conversion, on the other hand. During reaction the material irreversibly transforms from a chemically unstable initial mixture into a chemically (metastable) stable, partially cured polymer network or chain molecule. When the glass-transition temperature of the reaction mixture surpasses the reaction temperature $[T_g(t_{react}) \geq T_{react}]$ the material vitrifies. On the one hand, this vitrification affects the kinetics since molecular diffusion becomes extremely slow; on the other hand, the relaxation processes become very slow when the structure is frozen in a metastable, nonequilibrium state.

It is shown in Fig. 7 that the measured relaxation times tend to reach a limiting value when the reaction mixture vitrifies. The measured values of τ for a glassy system $[T_g(t_{react}) > T_{react}]$ are many orders of magnitude below those predicted by our simple equilibrium approach for relaxation during polymer network growth. The real relaxation is faster than the prediction of the equilibrium model.

For chemically stable materials the influence of the vitrification process on the thermal relaxation behavior is shown and its description by the fictive temperature is discussed [30, 31]. In analogy the description of the relaxation behavior during network formation demands a thermodynamic nonequilibrium approach. Since the freezing of structural relaxation during vitrification is not incorporated in the simple model considered here it applies only to the ideal liquid state. An approach incorporating the fictive temperature and the reduced time [32, 33] for modeling the nonequilibrium behavior of thermal relaxation is in progress.

Acknowledgements This work was supported by the Bundesminister für Wirtschaft through the Arbeitsgemeinschaft Industrieller Forschungsgemeinschaften grant no. 1154N. The authors wish to thank Werner Jenninger (Deutsches Kunststoff-Institut) for providing the dielectric data.

References

1. Prime RB (1997) In: Turi EA (ed) Thermal characterization of polymeric materials. Academic press, San Diego, pp 1380–1766
2. Gilham JK (1986) Polym Eng Sci 26:1429
3. Montserrat S (1992) J Appl Polym Sci 42:545
4. Gobrecht H, Hamann K, Willers G (1971) J Phys E Sci Instrum 4:21
5. Cassettari M, Salvetti G, Tombari E, Veronesi S, Johari GP (1992) Nuovo Cimento D 14:763
6. Ferrari C, Salvetti G, Tombari E, Johari GP (1996) Phys Rev E 54:R1058
7. Van Assche G, Van Hemelrijck A, Rahier H, Van Mele B (1995) Thermochim Acta 268:121
8. Sourour S, Kamal MR (1976) Thermochim Acta 14:41

9. Wisanrakkit G, Gillham JK (1990) J Appl Polym Sci 41:2885
10. Smith IT (1961) Polymer 2:95
11. Gallouedec F, Costa-Torro F, Laupretre F, Jasse B (1993) J Appl Polym Sci 47:823
12. Alig I, Nancke K, Johari GP (1994) J Polym Sci Polym Phys Ed 32:1465
13. Schawe JEK (2000) Thermochim Acta 361:97
14. Alig I, Jenninger W (1998) J Polym Sci Part B Polym Phys 36:2461
15. Menon N (1996) J Chem Phys 105: 5246
16. Birge NO, Dixon PK, Menon N (1997) Thermochim Acta 304/305:51
17. Vogel H (1921) Phys Z 22:645
18. Fulcher GS (1923) J Am Ceram Soc 8:339
19. Havriliak S, Negami S (1966) J Polym Sci C 14:99
20. Alig I, Lellinger D, Nancke K, Rizos A, Fytas G (1992) J Appl Polym Sci 44:829
21. Rozenberg BA (1985) Adv Polym Sci 75:113
22. Lunak S, Vladyka K, Dusek K (1978) Polymer 19:931
23. Pascault JP, Williams RJJ (1990) J Polym Sci Polym Phys Ed 28:85
24. DiBenedetto AT (1987) J Polym Sci Polym Phys Ed 25:1949
25. Kohlrausch R (1847) Ann Phys (Leipzig) 12:393
26. Williams G, Watts DC (1970) Trans Faraday Soc 66:80
27. Schlosser E, Kästner S, Friedland K-J (1981) Plaste Kautschuk 28:77
28. Parthun MG, Johari GP (1995) J Chem Phys 103:440
29. Alvarez F, Alegria A, Colmenero J (1993) Phys Rev B 47:125
30. Schawe JEK (1998) Colloid Polym Sci 276:565
31. Schawe JEK (1998) J Polym Sci Part B Polym Phys 36:2165
32. Tool AQ (1946) J Am Ceram Soc 29:240
33. Narayanaswamy OS (1971) J Am Ceram Soc 54:491